

Metal-catalyzed crystallization of amorphous carbon to graphene

Cite as: Appl. Phys. Lett. **96**, 063110 (2010); <https://doi.org/10.1063/1.3318263>

Submitted: 30 December 2009 . Accepted: 22 January 2010 . Published Online: 12 February 2010

Maxwell Zheng, Kuniharu Takei, Benjamin Hsia, Hui Fang, Xiaobo Zhang, Nicola Ferralis, Hyunhyub Ko, Yu-Lun Chueh, Yuegang Zhang, Roya Maboudian, and Ali Javey



View Online



Export Citation

ARTICLES YOU MAY BE INTERESTED IN

[Graphene segregated on Ni surfaces and transferred to insulators](#)

Applied Physics Letters **93**, 113103 (2008); <https://doi.org/10.1063/1.2982585>

[Raman Spectrum of Graphite](#)

The Journal of Chemical Physics **53**, 1126 (1970); <https://doi.org/10.1063/1.1674108>

[In situ x-ray diffraction study of graphitic carbon formed during heating and cooling of amorphous-C/Ni bilayers](#)

Applied Physics Letters **96**, 153105 (2010); <https://doi.org/10.1063/1.3397985>

Applied Physics Reviews
Now accepting original research

2017 Journal
Impact Factor:
12.894

Metal-catalyzed crystallization of amorphous carbon to graphene

Maxwell Zheng,^{1,2} Kuniharu Takei,^{1,2} Benjamin Hsia,³ Hui Fang,^{1,2} Xiaobo Zhang,^{1,2} Nicola Ferralis,³ Hyunhyub Ko,^{1,2} Yu-Lun Chueh,^{1,2} Yuegang Zhang,⁴ Roya Maboudian,^{2,3} and Ali Javey^{1,2,a)}

¹Department of Electrical Engineering and Computer Sciences, University of California, Berkeley, California 94720, USA and Materials Sciences Division, Lawrence Berkeley National Laboratory, Berkeley, California 94720, USA

²Berkeley Sensor and Actuator Center, University of California, Berkeley, California 94720, USA

³Department of Chemical Engineering, University of California, Berkeley, California 94720, USA

⁴The Molecular Foundry, Lawrence Berkeley National Laboratory, Berkeley, California 94720, USA

(Received 30 December 2009; accepted 22 January 2010; published online 12 February 2010)

Metal-catalyzed crystallization of amorphous carbon to graphene by thermal annealing is demonstrated. In this “limited source” process scheme, the thickness of the precipitated graphene is directly controlled by the thickness of the initial amorphous carbon layer. This is in contrast to chemical vapor deposition processes, where the carbon source is virtually unlimited and controlling the number of graphene layers depends on the tight control over a number of deposition parameters. Based on the Raman analysis, the quality of graphene is comparable to other synthesis methods found in the literature, such as chemical vapor deposition. The ability to synthesize graphene sheets with tunable thickness over large areas presents an important progress toward their eventual integration for various technological applications. © 2010 American Institute of Physics. [doi:10.1063/1.3318263]

Graphene has generated considerable interest in the recent years as a functional material for electronics, sensing, and energy applications^{1–4} owing to its unique electrical,^{5–7} optical,⁸ and mechanical⁹ properties. One critical challenge is the controlled synthesis of large-area graphene sheets. Recently, chemical vapor deposition (CVD) has been demonstrated as an attractive method to synthesize graphene.^{10–13} The precise control over the number of graphene layers is, however, difficult due to its sensitivity to various process parameters. In this regard, CVD scheme on Cu films has been shown to result in controlled synthesis of single-layer graphene.¹⁴ Here, we present a simple and efficient method to synthesize graphene layers via metal-catalyzed crystallization of amorphous carbon (a-C) by thermal annealing [Fig. 1]. In this process, the number of graphene layers is primarily dependent on the initial thickness of the a-C layer, resulting in highly controllable graphene synthesis.

The process involves the deposition of a layer of a-C (2.5–40 nm thick) by electron-beam evaporation on Si/SiO₂ substrates, followed by nickel or cobalt metal thin film (100–300 nm) deposition. The samples are then thermally annealed (650–950 °C) using a tube furnace under an argon flow and pressure of ~1.7 Torr. After cooling at a rate of ~20 °C/s, a graphitic layer is formed on the metal surface, as confirmed by Raman spectroscopy. Figure 2 shows the Raman spectra of the as-deposited a-C (~40 nm thick) and the resulting graphene layer after Ni-catalyzed crystallization at 800 °C for 15 min. The as-deposited carbon layer exhibits a broad Raman peak over the 1000–1700 cm⁻¹ range, indicative of a-C film. In contrast, the Raman spectrum after the Ni-catalyzed crystallization process exhibits the characteristic graphene fingerprints of D (~1395 cm⁻¹), G (~1580 cm⁻¹), and 2D (~2690 cm⁻¹) peaks [Fig. 2(b)].¹⁵

From the Raman spectrum, a ratio of D to G peaks, $I_D/I_G \sim 0.09$ with the 2D full width half maximum of ~51 cm⁻¹ are observed, indicating a multilayer graphene sheet with relatively low defect density, similar to the previously reported graphene sheets grown by CVD on Ni substrates.^{10–13}

The process mechanism is similar to that of the metal-induced crystallization of inorganic semiconductors which has been widely explored in the past.^{16,17} Briefly, in our case, carbon atoms diffuse into the metal layer at elevated temperatures followed by their precipitation as graphene on the free surface during the cool-down step as the solid solubility limit is reached. For a given annealing condition and cooling rate, the number of graphene layers is readily controlled by varying the thickness of the initially deposited a-C layer. This is an important difference between our “limited source” process and the CVD processes, where the carbon source is virtually unlimited and controlling the number of graphene layers depends on the tight control over a number of deposition parameters. Both nickel and cobalt proved to be suitable catalysts, whereas no graphene was formed when Cu thin film was used as the catalytic layer. This may be attributed to the low diffusivity and solid solubility limit of carbon in Cu.¹⁴

The annealing temperature is one important parameter that affects the metal-catalyzed crystallization process and the quality of the enabled graphene layer. As shown in Fig. 3, the graphene formation process is observed for annealing temperature in the range of 650–950 °C for Ni and

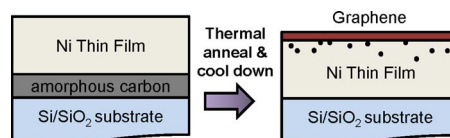


FIG. 1. (Color online) The process schematics for the metal-catalyzed crystallization of a-C to graphene by thermal annealing.

^{a)}Electronic mail: ajavey@eecs.berkeley.edu.

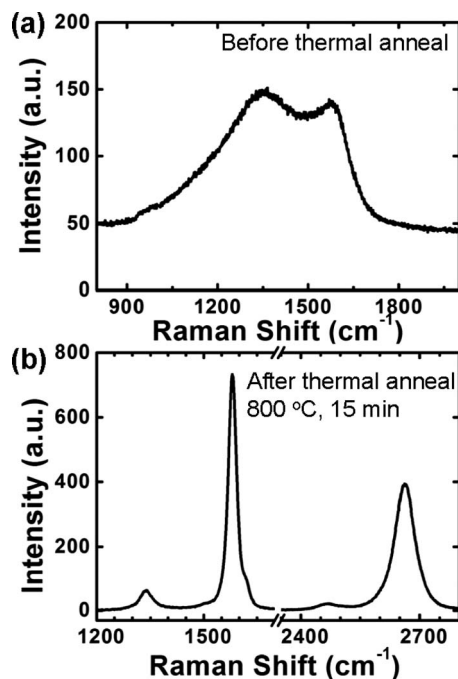


FIG. 2. Raman spectra of (a) a-C (40 nm) and (b) the resulting graphene layer after Ni-catalyzed crystallization (Ni thickness ~ 300 nm). Excitation laser wavelength was 632.8 nm.

650–850 °C for Co. From Raman analysis, the optimal temperatures for Ni and Co are ~ 800 and 750 °C, respectively. The anneal time is also systematically explored. Specifically, we observed the formation of graphene even when the samples (a-C thickness ~ 40 nm) were cooled down immediately after reaching the annealing temperature. Graphene formation and quality were found to be relatively indepen-

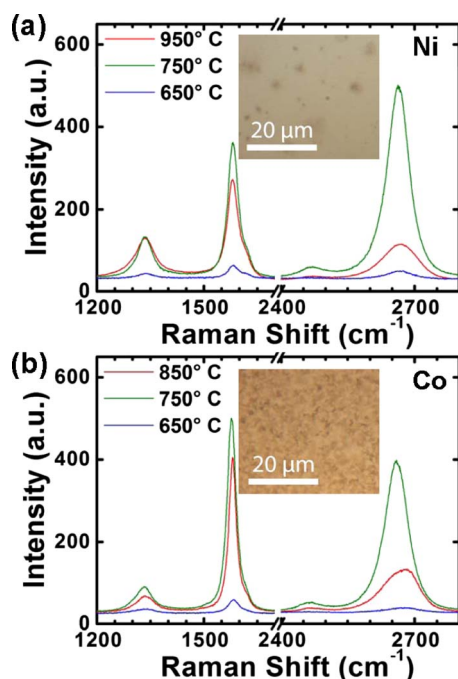


FIG. 3. (Color online) Raman spectra showing quality vs temperature dependence for (a) nickel catalyst and (b) cobalt catalyst. Graphene can form within a range of temperatures, although 750–800 °C appears to be optimal. Insets show representative optical images after annealing at 750 and 800 °C, showing relatively uniform surface coverage. The thickness of the initial a-C layer was 40 nm.

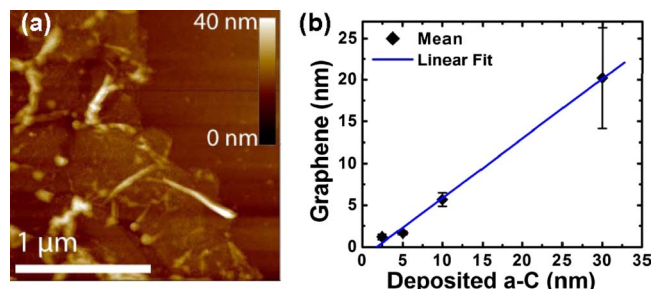


FIG. 4. (Color online) (a) AFM image of a transferred graphene sheet on a Si/SiO₂ substrate. (b) Graphene (and graphite) thickness vs initial a-C thickness. Samples were annealed at 800 °C for 15 min with a 300 nm Ni catalyst layer.

dent of the annealing time, up to ~ 60 min. For longer annealing times, the areas with graphene are notably reduced, and for annealing times > 5 hrs, no carbon or graphene are detected by Raman. This may be due to significant desorption of C atoms from the surface of the metal layer under the low pressure ambient.

The graphene layer formed on the metal film can be easily transferred to other substrates, which is an important factor for practical applications. Here, we have transferred the metal-crystallized graphene layer to Si/SiO₂ substrates by using a sacrificial poly(methyl methacrylate) (PMMA) layer as previously reported in literature.^{10–12} Briefly, after spin-coating a layer of PMMA onto the sample, the metal was etched away in 15% HCl solution and the detached film was placed in a water bath. Then, the film was transferred to a Si/SiO₂ substrate, allowed to dry, and placed in an acetone bath to dissolve the PMMA support layer. After a rinse with isopropyl alcohol, the samples were characterized. Alternatively, the graphene could be transferred without the use of PMMA. By placing the sample directly in HCl, the graphene layer detaches and floats, enabling easy retrieval and transfer.

The existence of graphene on the transferred Si/SiO₂ substrates was confirmed by Raman spectroscopy. No noticeable change in the Raman spectrum was observed after the transfer process. Subsequently, atomic force microscopy (AFM) was utilized to systematically investigate the thickness of precipitated graphene as a function of as-deposited a-C thin film by scanning the edges of transferred graphene sheets. Figure 4(a) shows a representative AFM image of a transferred graphene layer, showing the characteristic wrinkles and ripples,¹⁸ similar to the results obtained from other synthesis methods. Figure 4(b) shows the thickness of the crystallized graphene layer as a function of the deposited a-C film. The thickness of graphene shows a linear correlation with the thickness of the deposited carbon, with a slope of ~ 0.5 for an annealing temperature and time of 800 °C and 15 min, respectively. The results suggest that under these conditions and assuming equal densities of the as-deposited a-C and graphene, roughly half of the carbon source is crystallized into graphene with the rest either outgassing from the system or remaining in the Ni film. Notably, based on AFM and optical analyses, for the samples with initial a-C thickness of 2.5–5 nm, $\sim 70\%$ of the surface is covered with monolayer, $\sim 15\%$ is bilayer, and the rest consists of thick dendritic islands, which can be ten times as thick as the surrounding graphene. The exact mechanism for formation of these islands is unknown but these are possibly grain boundaries or crystal faces with energetically favorable sites

for multiple layers to form. The ability to tune the number of layers by the deposited a-C layer (i.e., limited source) presents a unique route toward controlled assembly and synthesis of graphene on large substrates, and presents an important advantage as compared to a CVD process where the C source is unlimited.

In conclusion, metal-catalyzed crystallization of a-C to graphene by thermal annealing is demonstrated. The thickness of the precipitated graphene is directly controlled by the thickness of the initial a-C layer. In addition, based on the Raman analysis, the quality is comparable to other synthesis methods found in the literature, such as CVD. In the future, by designing the metal-substrate interface properties, it may be possible to achieve the formation of graphene directly on the dielectric interface, which would further ease the fabrication complexity for device processing. Furthermore, the process temperature may also be lowered in the future by exploring various metal catalytic films, further enhancing the compatibility of this process with a wide range of substrates.

The authors acknowledge support from MSD Focus Center, Intel and NSF (Grant Nos. EEC-0832819 and CMMI-0825531). The fabrication part of this work was partially supported by the Molecular Foundry and a LDRD from LBNL. M.Z. acknowledges a SRC research scholarship.

- ¹A. K. Geim and K. S. Novoselov, *Nature Mater.* **6**, 183 (2007).
- ²X. Wang, L. Zhi, and K. Müllen, *Nano Lett.* **8**, 323 (2008).
- ³Y. Lin, K. A. Jenkins, A. Valdes-Garcia, J. P. Small, D. B. Farmer, and P. Avouris, *Nano Lett.* **9**, 422 (2009).
- ⁴A. K. Geim and P. Kim, *Sci. Am.* **298**, 90 (2008).
- ⁵S. V. Morozov, K. S. Novoselov, M. I. Katsnelson, F. Schedin, D. C. Elias, J. A. Jaszczak, and A. K. Geim, *Phys. Rev. Lett.* **100**, 016602 (2008).
- ⁶J. Chen, C. Jang, S. Xiao, M. Ishigami, and M. S. Fuhrer, *Nat. Nanotechnol.* **3**, 206 (2008).
- ⁷X. Wang, Y. Ouyang, X. Li, H. Wang, J. Guo, and H. Dai, *Phys. Rev. Lett.* **100**, 206803 (2008).
- ⁸R. R. Nair, P. Blake, A. N. Grigorenko, K. S. Novoselov, T. J. Booth, T. Stauber, N. M. R. Peres, and A. K. Geim, *Science* **320**, 1308 (2008).
- ⁹C. Lee, X. Wei, J. W. Kysar, and J. Hone, *Science* **321**, 385 (2008).
- ¹⁰Q. Yu, J. Lian, S. Siriponglert, H. Li, Y. P. Chen, and S. Pei, *Appl. Phys. Lett.* **93**, 113103 (2008).
- ¹¹A. Reina, X. Jia, J. Ho, D. Nezich, H. Son, V. Bulovic, M. S. Dresselhaus, and J. Kong, *Nano Lett.* **9**, 30 (2009).
- ¹²K. S. Kim, Y. Zhao, H. Jang, S. Y. Lee, J. M. Kim, K. S. Kim, J. Ahn, P. Kim, J. Choi, and B. H. Hong, *Nature (London)* **457**, 706 (2009).
- ¹³L. G. De Arco, Y. Zhang, A. Kumar, and C. Zhou, *IEEE Trans. Nanotechnol.* **8**, 135 (2009).
- ¹⁴X. Li, W. Cai, J. An, S. Kim, J. Nah, D. Yang, R. Piner, A. Velamakanni, I. Jung, E. Tutuc, S. K. Banerjee, L. Colombo, and R. S. Ruoff, *Science* **324**, 1312 (2009).
- ¹⁵A. Ferrari, J. Meyer, V. Scardaci, C. Casiraghi, M. Lazzeri, F. Mauri, S. Piscanec, D. Jiang, K. Novoselov, S. Roth, and A. Geim, *Phys. Rev. Lett.* **97**, 187401 (2006).
- ¹⁶J. Hamilton and J. Blakely, *Surf. Sci.* **91**, 199 (1980).
- ¹⁷W. Knaepen, C. Detavernier, R. V. Meirhaeghe, J. J. Sweet, and C. Lavoie, *Thin Solid Films* **516**, 4946 (2008).
- ¹⁸A. Fasolino, J. H. Los, and M. I. Katsnelson, *Nature Mater.* **6**, 858 (2007).